ANTIOXIDANTS & REDOX SIGNALING
Volume 7, Numbers 11 & 12, 2005

Forum Original Research Communication

Nitric Oxide Synthases Modulate Progenitor and Resident Endothelial Cell Behavior in Galactosemia

E. ANN ELLIS,[1] NILANJANA SENGUPTA,[2] SERGIO CABALLERO,[2] STEVEN M. GUTHRIE,[3] ROBERT N. MAMES,[4] and MARIA B. GRANT[2]

ABSTRACT

We used knockout animals of either inducible nitric oxide synthase (iNOS$^{-/-}$) or endothelial NOS (eNOS$^{-/-}$) to characterize the role of NOS in galactosemia, a model of diabetic retinopathy. NADH oxidase and nitrotyrosine were used as biomarkers of oxidative stress and vascular dysfunction. These animals were engrafted with hematopoietic stem cells (HSC) expressing green fluorescence protein (gfp^{+}) to characterize the contribution of HSC and endothelial progenitor cells to neovascularization. Increased NADH oxidase activity and superoxide generation occurred in all galactose-fed mice. eNOS$^{-/-}$ mice demonstrated increased iNOS immunoreactivity in their retinal vasculature. Nitrotyrosine levels were low at baseline in the wild-type (WT) mice, eNOS$^{-/-}$ and iNOS$^{-/-}$ mice, and the galactose-fed iNOS mice and increased following galactose feeding in eNOS$^{-/-}$ and WT. Galactose-fed WT.gfp and iNOS$^{-/-}$.gfp chimeric animals had areas of perfused new vessels composed of gfp^{+} cells. In contrast, galactose-fed eNOS$^{-/-}$.gfp mice produced copious, unbranched, nonperfused tubes. Thus, nitric oxide modulates HSC behavior and vascular phenotype in the retina. Although there is increased NADH oxidase and superoxide in galactosemic mice of all isoforms, iNOS is the source of nitric oxide responsible for peroxynitrite and nitrotyrosine formation that leads to the pathology observed in galactosemic mice. *Antioxid. Redox Signal*. 7, 1413–1422.

INTRODUCTION

NITRIC OXIDE (NO) has been implicated in the pathophysiology of diabetic vascular complications. NO is a gaseous free radical that induces vasodilatation, prevents platelet aggregation and leukocyte adhesion, and promotes synaptic transmission and cytostatic/cytotoxic actions in macrophages (21, 28). NO arises from the guanidino group of L-arginine and is catalyzed by a family of nitric oxide synthases (NOS). Isoforms of NOS derived from separate genes are neuronal NOS (nNOS, NOS1), inducible NOS (iNOS, NOS2), and endothelial NOS (eNOS, NOS3). The three isoforms are similar in structure and function, utilizing L-arginine, oxygen, and NADPH as substrates, and requiring FAD, FMN, calmodulin, and tetrahydrobiopterin as cofactors. The catalytic mechanism of NOS involves flavin-mediated electron transport from NADPH to the terminal heme, where oxygen is bound and incorporated into NO and citrulline (39).

In diabetes, NO production may not be reduced, but may just not be available because of inactivation by excessive NO production of superoxide ($O_2^{\cdot -}$) in the vascular wall. The effects of NO depend on its microenvironment, and one mechanism for its role in complications of diabetes is the reaction with $O_2^{\cdot -}$ to form the toxic species peroxynitrite ($ONOO^-$). This reaction occurs at near diffusion-limited rates and is more than three times faster than the enzymatic dismutation of $O_2^{\cdot -}$ by superoxide dismutase (SOD) (3). Several studies have demonstrated elevated levels of NO associated with vascular

[1]Microscopy and Imaging Center, Texas A&M University, College Station, TX.
[2]Department of Pharmacology and Therapeutics, University of Florida, Gainesville, FL.
[3]Program in Stem Cell Biology, University of Florida, Gainesville, FL.
[4]The Retina Center, Gainesville, FL.

dysfunction in diabetes through increased formation of $ONOO^-$, including disruption of the blood–retinal barrier (BRB) (6, 15, 25, 41). $ONOO^-$ is a potent volatile oxidant that can attack many types of biological molecules. High levels of $ONOO^-$ initiate lipid peroxidation, hydrooxidation, nitration of amino acids such as tyrosine, and oxidation of antioxidants such as ascorbic acid and α-tocopherol, and can cause direct DNA damage.

Hyperglycemia in diabetes results in a shift of metabolism to the polyol/sorbitol pathway where it increases cytosolic NADH/NAD and creates a "pseudohypoxia" in the presence of normal oxygen levels (42). The $O_2^{\cdot -}$ radical dismutates, either spontaneously or catalyzed by SOD, to yield hydrogen peroxide (H_2O_2). NADH oxidase has been demonstrated to be the major source of reactive oxygen species (ROS) in vascular endothelium (26, 27, 34), and a number of investigations have demonstrated increased NADH oxidase in diabetes. High glucose increased levels of NADH oxidase and $O_2^{\cdot -}$ in cultured vascular cells and coronary arteries (8), and specific inhibitors of NADH oxidase blocked the increases in $O_2^{\cdot -}$. Vascular NADH oxidase was shown to be involved in impaired endothelium-dependent vasodilatation in the OLETF rat model of non–insulin-dependent diabetes mellitus (NIDDM) (24), and diphenyleneiodonium (DPI) inhibited the increase in $O_2^{\cdot -}$. More recently, there is additional evidence of vascular NADH oxidase contributing to increased oxidative stress in animal models of diabetes associated with obesity (40). Our work with the BBZ/Wor rat, a model of type II diabetes, showed increased cytochemical localization of NADH oxidase confined to the vascular endothelium in diabetic retinopathy (12, 13). The localization was blocked by DPI, as well as by removal of the substrate NADH; allopurinol, a specific inhibitor of xanthine oxidase, did not block the localization (13).

Previously, we showed a significant increase in NADH oxidase, a marker of oxidative stress, in the retinal vessels of a rat model of NIDDM. Eighty percent of vessels were reactive for H_2O_2 compared with only 38% of vessels in nondiabetic rats. Areas of H_2O_2 localization corresponded to BRB dysfunction (12), increased vascular endothelial growth factor (VEGF) expression (13), and increased iNOS and nitrotyrosine (14), which is an indication of $ONOO^-$ formation (4). $ONOO^-$ has been implicated in vascular permeability in experimental diabetes (15). Tyrosine nitration can adversely affect various cellular metabolic and signaling processes and may directly contribute to development of endothelial cell dysfunction.

A number of studies have documented a role for NO in diabetic retinopathy. Hyperglycemia has been shown to suppress eNOS in retinal vascular endothelial cells (7). Recent studies with Goto–Kakizaki rats, a model of NIDDM, demonstrated expression of iNOS in the retina by western analysis, immunohistochemistry, and inhibition by NOS inhibitors (6). In addition, western analysis of retinas from rats with streptozotocin-induced diabetes showed expression of iNOS and nitrotyrosine (10). Cultures of bovine retinal endothelial cells incubated in 25 m*M* glucose had increases in NO, iNOS, and nitrotyrosine (10). Previously, we performed time-course studies of hyperglycemia and oxidative stress in the BBZ/Wor rat and demonstrated an increase in nitrotyrosine in the retinal vessels of these diabetic rats from the onset of hyperglycemia (14).

Retinal endothelium is strongly positive for NO. The production of NO by retinal endothelium that has been observed is consistent with a role for NO in mediating endothelial cell behavior. Retinal endothelial cells in culture constitutively express significant amounts of Ca^{2+}-dependent eNOS activity, in addition to being induced by cytokines to produce iNOS (20). ROS play a role in retinal ischemia and proliferative retinopathy (20). The burst of $O_2^{\cdot -}$ as a result of reperfusion can be generated from vascular NADH oxidase (16), as well as neutrophil-derived NADPH oxidase (31). NADH oxidase has been demonstrated as a source of ROS in hypoxia (17). This excess of $O_2^{\cdot -}$ can react with NO from the vascular endothelium to form $ONOO^-$ and may play a role in endothelial dysfunction in proliferative retinopathy. Therefore, changes in levels of either iNOS or eNOS in the endothelium may lead to endothelial dysfunction.

In this study, we examined the hypothesis that increased levels of NO generated by iNOS as observed in the $eNOS^{-/-}$ mice are injurious to the retinal vasculature and that the injury may be due to $ONOO^-$. Isoform-specific knockouts of NOS allowed the examination of the loss of functional behavior of each enzyme in the physiological context of an intact animal without the use of pharmacological inhibitors that are not entirely selective (37). Experimental galactosemia, which is associated with increased levels of ROS, induces a diabetic-like retinopathy (22, 23, 36), and branch vein occlusion induces neovascularization (18). The effect of systemic deficiency of NOS isoforms on the behavior of endothelial precursor cells (EPC) was examined by reconstituting $iNOS^{-/-}$ and $eNOS^{-/-}$ animals with bone marrow from green fluorescent protein (gfp) homozygous animals. We show that NO can modulate hematopoietic stem cell (HSC) behavior and vascular phenotype in the retina and that iNOS is the source of NO responsible for $ONOO^-$ and nitrotyrosine formation that leads to the pathology observed in galactosemic mice.

MATERIALS AND METHODS

Animals

All animal care and procedures conformed to the Association for Research in Vision and Ophthalmology Resolution on the Use of Animals in Research and NIH guidelines on the use of animals in research. All procedures were approved by the Institutional Animal Care and Use Committee.

Six groups of mice were utilized in this study: nongalactosemic and galactosemic $eNOS^{-/-}$ mice, nongalactosemic and galactosemic $iNOS^{-/-}$ mice, and nongalactosemic and galactosemic wild-type (WT) mice. Breeding pairs of C57BL6/J (WT), B6.129P2-Nos3^{tm1Unc}/J ($eNOS^{-/-}$), and B6.129P2-Nos2^{tm1Lau}/J ($iNOS^{-/-}$) were purchased from Jackson Laboratories (Bar Harbor, ME, U.S.A.). Mice were weaned at 4 weeks of age onto Purina rodent chow (Ralston Purina, St. Louis, MO, U.S.A.) and water *ad libitum*. At 8 weeks of age, male mice were divided into two groups: the control group of each strain was maintained on Purina rodent chow; the second group was

switched to Purina rodent chow that contained 30% galactose (Purina Mills, Richmond, IN, U.S.A.). Four and 12 weeks later, mice were euthanized with an overdose of 0.1 ml of ketamine/xylazine (100 mg/ml ketamine + 20 mg/ml xylazine). Blood samples were obtained at euthanasia, and whole-blood glucose was measured using a Glucometer Elite Glucose Meter (Bayer Diagnostic Division, Tarrytown, NY, U.S.A.).

Immunohistochemical localization of eNOS and iNOS

WT, iNOS$^{-/-}$, and eNOS$^{-/-}$ mice were perfused with 3–6 ml of 4% paraformaldehyde in phosphate-buffered saline (PBS). Both eyes from each animal were enucleated, pierced with a 27-gauge needle 1 mm posterior to the limbus, incubated in 4% paraformaldehyde for 30 min, and then washed in PBS for at least 30 min. The neural retina was then dissected from the retinal pigment epithelium (RPE)/choroid/sclera complex. Whole retinas were permeabilized and blocked in HEPES-buffered saline containing 0.2% (vol/vol) Triton X-100, 0.2% (wt/vol) bovine serum albumin, 0.2% (vol/vol) rabbit serum, and 0.2% (vol/vol) goat serum (all from Sigma–Aldrich, St. Louis, MO, U.S.A.) for 3 hours at room temperature. After 3 h, either rabbit anti-iNOS (1:50; Abcam, Cambridge, MA, U.S.A.) or rabbit anti-eNOS (1:50; BD–Pharmingen, San Diego, CA, U.S.A.) was added along with rhodamine-conjugated *Ricinus communis* agglutinin (1:1,000; Vector Laboratories, Burlingame, CA, U.S.A.) and incubated for 24 h at 4°C. The tissues were washed in HEPES-buffered saline, then placed in 1:800 biotinylated goat anti-rabbit IgG (Sigma–Aldrich) in PBS for 24 h at 4°C, followed by a wash in PBS for 24 h at 4°C. Lastly, the tissues were placed in 1:50 streptavidin–fluorescein isothiocyanate (FITC) in bicarbonate buffer (Vector Laboratories) for 24 h and then washed for 24 h at 4°C in bicarbonate buffer. As controls, at least one retina from each of the three types of animals was not placed into the primary antibody, but was incubated with secondary antibody followed by streptavidin-FITC as previously described (18).

After the final wash, each retina was flat-mounted with four to seven radial cuts (38) and imaged using a Zeiss RGB Spot CCD camera coupled to an Axioplan 2 fluorescence microscope with filters for FITC and rhodamine, as well as bright field. Captured digital images for the red and green channels were then merged to show colocalization of NOS isoforms (FITC-labeled) with vascular tissue (rhodamine-labeled).

Cytochemical localization of NADH oxidase

Eyes were enucleated and fixed for 1 h in cold 5% acrolein (vol/vol) in 0.1 *M* sodium cacodylate-HCl buffer (pH 7.4). Specimens were washed 4 × 15 min in 0.15 *M* sodium cacodylate buffer (pH 7.4) plus 5% (wt/vol) sucrose and 1% (vol/vol) dimethyl sulfoxide. Tissue was held in the cold in buffer wash until it was reacted for NADH oxidase cytochemical localization.

Specimens were brought to room temperature in the final two buffer washes, which contained 0.1 *M* glycine, and then preincubated for 30 min at 37°C with agitation in the following medium: 2.0 m*M* cerium chloride, 10 m*M* 3-amino-1,2,4-triazole, 0.1 *M* Tris-maleate buffer (pH 7.5), 7% sucrose, and 0.0002% Triton X-100. They were then incubated in the following complete reaction medium: 2.0 m*M* cerium chloride, 10 m*M* 3-amino-1,2,4-triazole, 0.8 m*M* NADH, 0.1 *M* Tris-maleate buffer (pH 7.5), 7% sucrose, and 0.0002% Triton X-100 for 2 × 30 min at 37°C with agitation. The reaction was terminated by washing in cold 0.15 *M* Tris-maleate buffer (pH 7.5), 7% sucrose, followed by a wash in cold 0.15 *M* sodium cacodylate-HCl buffer (pH 7.4), 7% sucrose. Specificity of the reaction was demonstrated by the following: (a) omitting NADH; (b) using an inhibitor of NADH oxidase, 1.0 m*M* DPI; and (c) using an inhibitor of xanthine oxidase, 1.0 m*M* allopurinol. Specimens were then postfixed overnight in 1% (wt/vol) osmium tetroxide, dehydrated, infiltrated, and embedded as previously described (12, 13). Grids were examined and photographed at 75 kV in a Hitachi H-7000 transmission electron microscope.

Immunocytochemical localization of nitrotyrosine

Sections from eyes in which NADH oxidase had been localized were picked up on nickel grids; oxidized 30 min with 1% (wt/vol) periodic acid, followed by 5 × 5-min washes in deionized water. Grids were floated 2 × 5 min on PBS (pH 7.2), followed by 30 min on PBS blocker [PBS + 2% (wt/vol) cold water fish gelatin (Sigma–Aldrich)], and then reacted overnight at 4°C in a moist chamber with rabbit anti-nitrotyrosine antibodies (Upstate Biotechnology, Lake Placid, NY, U.S.A.) diluted to 10 µg/ml with PBS blocker. After 2 × 5-min washes with PBS blocker followed by 2 × 5-min washes with PBS, grids were washed with Tris-HCl saline buffer (TBS, pH 7.6) followed by 30 min on TBS blocker (TBS + 2% cold water fish gelatin). Grids were then incubated for 1 h at room temperature in a moist chamber on drops of donkey anti-rabbit IgG labeled with 18-nm colloidal gold (Jackson Immunoresearch Laboratories Inc., West Grove, PA, U.S.A.) diluted 1:40 with TBS blocker. Grids were washed with TBS blocker, followed by 2 × 5-min washes with TBS and then 3 × 5-min washes with deionized water. Control grids were incubated with only the gold labeled with secondary antibody or with primary antibodies that had been absorbed overnight with an excess of nitrated protein (Upstate Biotechnology).

Morphometric analysis

Quantitation of NADH oxidase localization was done by a modification of the method of Briggs *et al.* (5). Sections examined included the neural retina and choroid ~1 mm on either side of the optic nerve head. All blood vessels in the retina were examined at a magnification of 10,000× and scored either positive (cerium perhydroxide was present in any of the following sites: vessel lumen, endothelial cell cytoplasm, plasmalemma, basement membrane) or negative (cerium perhydroxide was absent). Results were expressed as the percentage of positive vessels relative to the total number of vessels examined for each grid. For quantitation of nitrotyrosine immunolocalization, blood vessels were examined at a magnification of 10,000×. Twenty vessels in one eye of each of four galactose-fed and four age-matched control mice in each of the groups were sampled. Counts of colloidal gold

particles were normalized to a standard area of 50 μm^2. The sections used for immunocytochemical localization of nitrotyrosine were serial sections of the same area in which quantitative studies of NADH oxidase cytochemical localization had been done.

Generation of iNOS$^{-/-}$ and eNOS$^{-/-}$ gfp$^+$ chimeric mice

Chimeric animals were produced by irradiating recipient mice (WT with 950 rads, iNOS$^{-/-}$ and eNOS$^{-/-}$ with 650 rads), followed by intravenous transplant of up to 2,500 Sca-1$^+$, c-kit$^+$, lineage-negative *gfp*$^+$ HSC. The difference in radiation doses is due to the increased sensitivity of the knockout animals to radiation. It was found that 950 rads proved lethal to a high proportion of the eNOS$^{-/-}$ animals. HSC were isolated and transplanted as previously described (18).

Induction of retinal neovascularization in chimeric mice

Long-term durable hematopoietic reconstitution was confirmed by flow cytometry analysis of peripheral blood 3 and 6 months post transplant. Cohorts (n = 0) were identified with similar engraftment rates of peripheral blood mononuclear cells (all >70% donor-derived when normalized to donor gfp$^+$ animals) for subsequent experimentation. Matched cohorts were injected with saturating titers (1×10^9 PFU) of recombinant adeno-associated virus (rAAV; VectorCore, University of Florida) expressing the full-length human $VEGF_{165}$ directly into the vitreous using a 36-gauge needle and Hamilton syringe. The dosage was determined by *in vivo* titering for maximal HSC response. We had previously determined that site-specific expression of VEGF prior to branch retinal vessel photocoagulation was necessary to achieve consistent preretinal neovascularization characteristic of what is seen in proliferative diabetic retinopathy (18). One month after viral infection, the mice underwent laser treatment. An argon green indirect ophthalmic laser system (HGM Corp., Salt Lake City, UT, U.S.A.) was used for retinal vessel photocoagulation (80–100 burns) with the aid of a 78-diopter lens as previously described (18). The combination of growth factor overexpression and ischemic injury mimics to some extent the ocular diabetic milieu, and results in the formation of preretinal neovascular tufts similar to those seen in proliferative diabetic retinopathy. One important difference between this model and proliferative diabetic retinopathy is that the animals, lacking the many cellular and molecular dysregulations associated with diabetes, are able to resolve the ocular neovascularization by 6 weeks post laser. Three weeks after laser injury, at the time of typically maximal neovascularization in this model, the animals were euthanized and perfused with 50 mg/ml rhodamine-conjugated dextran in 4% paraformaldehyde in PBS (Sigma–Aldrich). Eyes were enucleated and the neural retinas dissected and mounted flat for imaging by epifluorescence microscopy as described earlier. Selected retinas were also imaged by laser scanning confocal microscopy to determine the location of the vessels within the neural retina.

Statistical analysis

One-way ANOVA was used to compare response variable means among the WT, iNOS$^{-/-}$, and eNOS$^{-/-}$ groups. Analysis of covariance (ANCOVA) was used to compare the age-adjusted mean percentage of retinal changes testing positive for qualitative histological changes between control and galactose animal groups. Individual animal percentages were arcsine-square root transformed prior to analysis to stabilize variances, and a weighted ANCOVA was fitted to account for variation in the total number of vessels assessed per retina.

RESULTS

Immunohistochemical localization of eNOS and iNOS

In each knockout strain, the isoform that is genetically deleted is not expressed *in vivo* at detectable levels, nor is eNOS expressed in detectable levels in the iNOS$^{-/-}$ animals. However, the retinas of eNOS$^{-/-}$ animals demonstrate iNOS immunoreactivity (Fig. 1). This suggests that there is compensatory up-regulation of iNOS expression in eNOS knockout retinas, indicating NOS dysregulation and a large amount of NO produced.

Nitrotyrosine and NADH oxidase in galactose-fed animals

Table 1 shows the mean weights and blood glucose levels of the animals and contrasts those values for the normal diet versus galactose-fed mice. All of the galactose-fed animals exhibited nearly a twofold increase in blood glucose compared with normal animals. Furthermore, the galactose-fed animals were not significantly heavier than normal animals, indicating a "diabetes-like" state not attributable to obesity.

NADH oxidase, a marker of oxidative stress and the major source of $O_2^{\cdot -}$ in the vascular endothelium, localized primarily in endothelial cells and pericytes (Fig. 2 and Table 2). NADH oxidase activity was increased in retinal capillaries of all three groups of galactose-fed mice (Table 2). However, nitrotyrosine increased threefold in the galactose-fed WT mice and sevenfold in the galactose-fed eNOS$^{-/-}$ mice, whereas

Table 1. Average Weight and Blood Glucose in WT (C57BL/6J), eNOS$^{-/-}$, and iNOS$^{-/-}$ Mice Being Fed a Normal Diet or a Galactose-Rich Diet for 3 Months

Mouse group	*Weight (g)*	*Blood glucose (mg/dl)*
C57BL/6J		
Normal diet	27.3 ± 0.84	183 ± 26
30% galactose	22.6 ± 1.07	332 ± 55
eNOS$^{-/-}$		
Normal diet	28.6 ± 2.40	175 ± 11
30% galactose	24.9 ± 0.45	324 ± 15
iNOS$^{-/-}$		
Normal diet	26.3 ± 0.65	168 ± 18
30% galactose	25.5 ± 2.28	300 ± 26

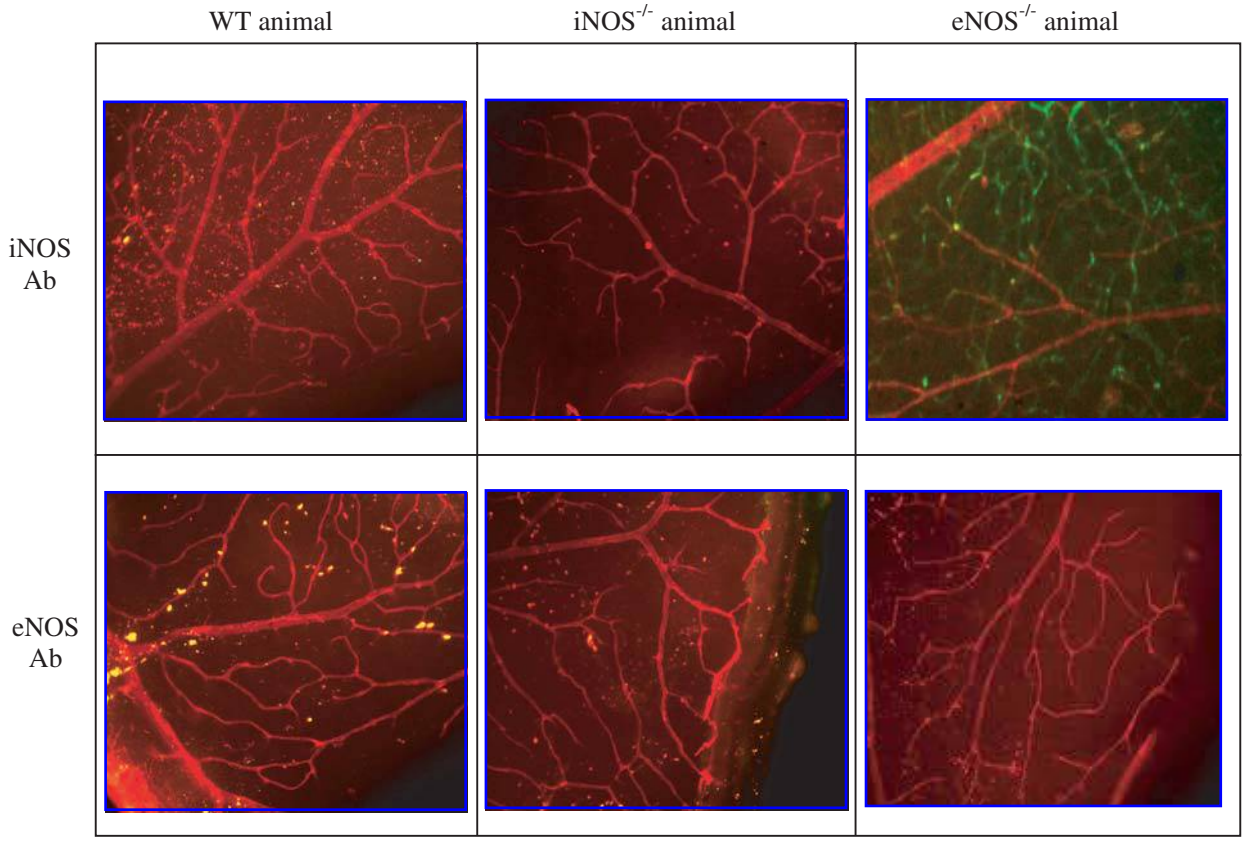

FIG. 1. Fluorescence micrographs of immunohistochemistry studies show neural retinas from WT, iNOS$^{-/-}$, and eNOS$^{-/-}$ animals. Red fluorescence defines rhodamine-agglutinin labeling of the vasculature; green fluorescence shows FITC-labeled iNOS or eNOS antibody (Ab). As controls, tissues from an iNOS$^{-/-}$ animal and an eNOS$^{-/-}$ animal were reacted with iNOS antibody and eNOS antibody, respectively. These tissues do not show any specific labeling of the antibody. Tissue from WT animals also did not show specific antibody binding with either the iNOS antibody or the eNOS antibody. When tissue from an iNOS$^{-/-}$ animal was reacted with eNOS antibody, no antibody labeling was seen. However, when the neural retina from an eNOS$^{-/-}$ animal was reacted with iNOS antibody, there was intense fluorescence and specific colocalization of iNOS in the vasculature.

TABLE 2. NADH OXIDASE AND NITROTYROSINE QUANTITATION IN WT (C57BL/6J), eNOS$^{-/-}$, AND iNOS$^{-/-}$ MICE BEING FED A NORMAL DIET OR A GALACTOSE-RICH DIET FOR 3 MONTHS

Mouse group	*Percentage of vessels positive for NADH oxidase*	*Nitrotyrosine localization (gold particles/ 50 μm²)*
C57BL/6J		
Normal diet	50.1 ± 7.72%	10.7 ± 3.80
30% galactose	85.0 ± 7.07%*	32.7 ± 5.36†
eNOS$^{-/-}$		
Normal diet	41.1 ± 12.66%	5.45 ± 3.71
30% galactose	81.9 ± 7.22%*	38.0 ± 10.29†
iNOS$^{-/-}$		
Normal diet	49.5 ± 1.41%	8.05 ± 3.98
30% galactose	72.0 ± 1.10%*	10.6 ± 4.27

Note that galactose-fed iNOS$^{-/-}$ animals did not show an increase in nitrotyrosine, in contrast to either WT or eNOS$^{-/-}$ animals.

*$p < 0.05$.

†$p < 0.01$.

the galactose-fed iNOS$^{-/-}$ mice showed no increase in nitrotyrosine above basal levels. WT and eNOS$^{-/-}$ mice fed galactose showed disruption of the basal infoldings of the RPE. The iNOS$^{-/-}$ mice fed galactose were protected from the development of these RPE changes.

EPC involvement in retinal neovascularization

The iNOS$^{-/-}$.gfp mice demonstrated small discrete areas of predominantly preretinal, with some intraretinal, neovascularization similar in size and distribution to the WT.gfp mice used as controls (Fig. 3A), and differing in no respect from previously reported observations (18). These new vessels—identified by their "yellow" fluorescence on merged red and green channel images—demonstrated vessel patency by virtue of their perfusability with rhodamine-conjugated dextran. In addition, they were composed of gfp^{+} cells, indicating that these were new vessels formed by cells that differentiated from bone marrow precursors.

In contrast, the eNOS$^{-/-}$.gfp chimeric mice demonstrated numerous areas of nonperfused capillaries located preretinally (Fig. 3B). The overall appearance of these "vessels," in both

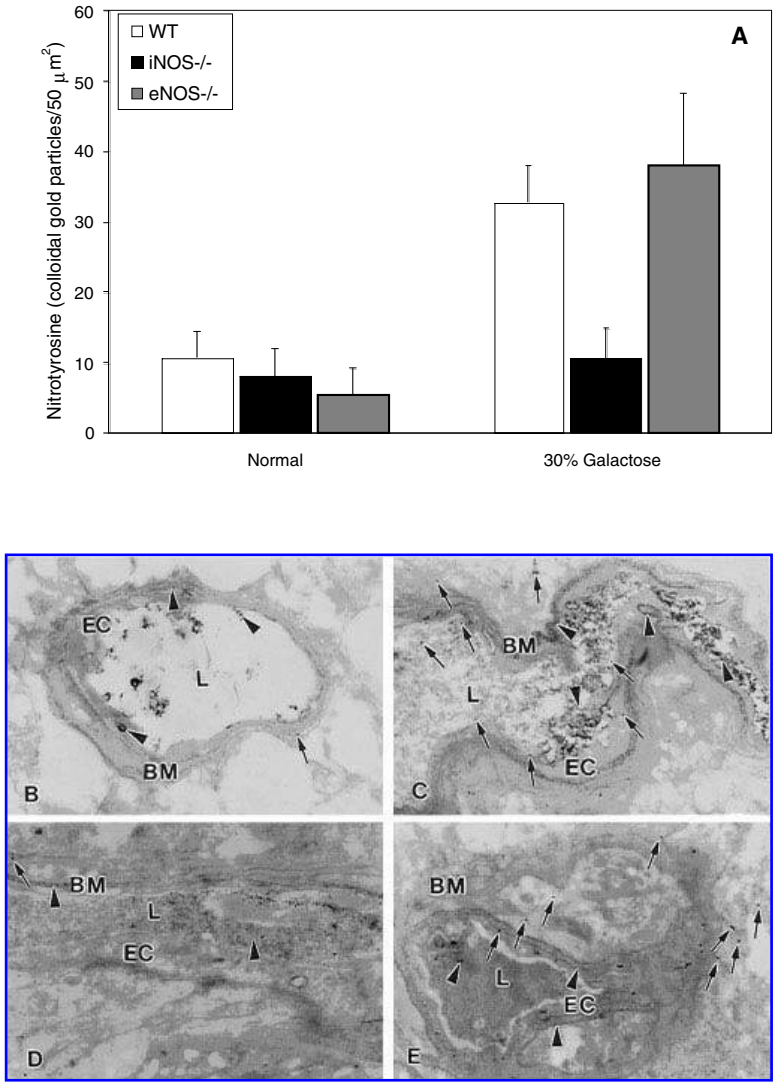

FIG. 2 (**A**) Graphical representation of the quantification data for nitrotyrosine in the three mouse strains fed a normal or galactose-rich diet. (**B**) Localization of nitrotyrosine (arrows) and NADH oxidase (arrowheads) in retina of C57BL/6J (WT) mouse on normal diet. (**C**) Nitrotyrosine and NADH oxidase localization in retina of WT mouse fed 30% galactose diet for 1 month. (**D**) Localization of nitrotyrosine and NADH oxidase in retina of iNOS$^{-/-}$ mouse fed 30% galactose diet for 1 month. (**E**) Localization of nitrotyrosine and NADH oxidase in retina of eNOS$^{-/-}$ mouse fed 30% galactose diet for 1 month. BM, basement membrane; EC, endothelial cell; L, vessel lumen. All micrographs: ×10,000.

frequency and structure, is atypical of neovasculature seen in WT or iNOS$^{-/-}$ mice undergoing the same growth factor–retinal vessel occlusion model. The vessels in the eNOS$^{-/-}$.gfp animals are composed entirely of gfp^{+} cells, and thus derived from bone marrow precursors. However, these vessels were not patent because no rhodamine-conjugated dextran was found to perfuse through them. Additionally, the structure of these neovascular areas lacked the branching typical of neovascular tufts found in the WT and iNOS$^{-/-}$ animals.

DISCUSSION

The purpose of these studies was to examine hemangioblast function in a setting of increased oxidative and increased nitrosative stress. Galactosemia was used as way to increase oxidative stress, and the NOS knockout mice were used to manipulate endogenous NO levels. From the experiments conducted, we conclude that there appears to be an isoform-specific role for NOS in the retinal pathology observed with galactosemia and laser-induced neovascularization. Although neither model is identical to diabetes, galactosemia induces retinal changes typically associated with diabetes, such as basement membrane thickening, pericyte loss, and acellular capillaries, and the laser model causes ischemia resulting in preretinal neovascularization. Both galactosemia and laser-induced vessel occlusion are associated with activation of NADPH oxidase (11, 31). iNOS$^{-/-}$.gfp and eNOS$^{-/-}$.gfp chimeric mice were utilized to characterize the contribution of WT HSC and EPC to the correction of vascular dysfunction in these knockout mice. The absence of iNOS as observed in the iNOS$^{-/-}$ mice protected against the development of retinal pathology and resulted in reduced generation of nitrotyrosine following long-term galactose feeding, whereas eNOS$^{-/-}$ mice fed galactose showed an increase in nitrotyrosine and progressive retinal pathology. In the laser injury model, the eNOS$^{-/-}$.gfp chimeric mice showed more dramatic incorporation of gfp^{+} cells in retinal blood vessels, whereas the iNOS$^{-/-}$ mice responded in a less dramatic manner, similar to the WT.

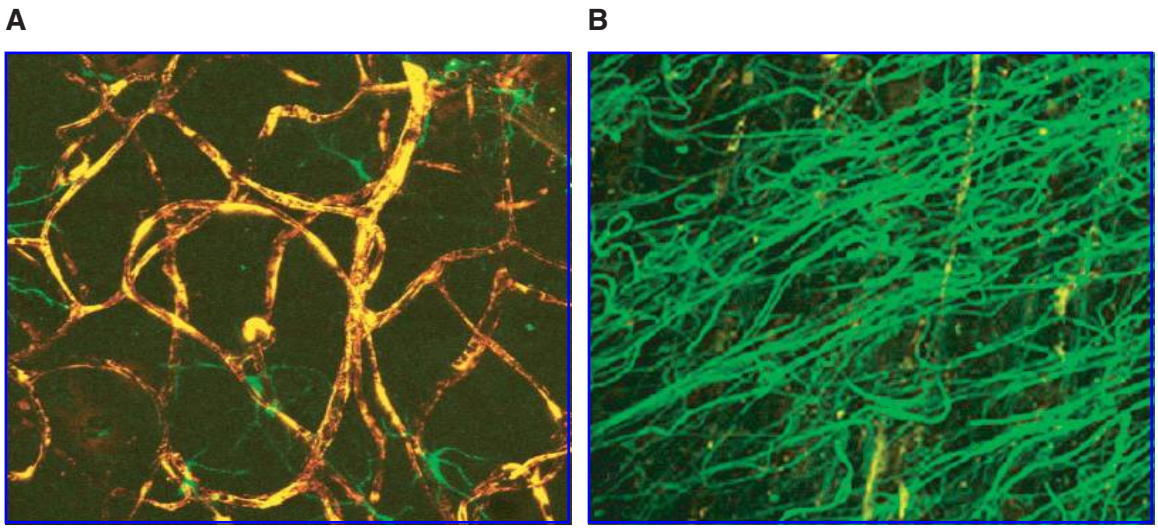

FIG. 3. Mice were transplanted with gfp$^+$ donor stem cells that were Sca-1$^+$, c-kit$^+$, Lin$^-$ (*i.e.,* HSC), and then neovascularization was induced by VEGF overexpression, followed by ischemic insult in the form of branch retinal vessel photocoagulation. (**A**) Typical neovascular tuft from an iNOS$^{-/-}$.gfp animal. Yellow fluorescence indicates perfusable vessels composed of gfp$^+$ cells. The vessel architecture is typical of what is seen in WT animals treated in an identical fashion. (**B**) Neovascular area on the retina of an eNOS$^{-/-}$.gfp animal is shown and is typical of the abnormal, nonperfused vessels seen. Note the high density, tortuosity, and lack of branching in the nonperfused green blood vessels in these animals. Original magnification of both micrographs was ×40.

We postulate an increase in nitrotyrosine in the retinal vasculature in eNOS$^{-/-}$ mice at the time the retina is made ischemic by laser treatment. This ischemia could release a cascade of $O_2^{\cdot -}$ from NADH oxidase due to hypoxia (17), and increased NO is present because iNOS is over expressed in the eNOS$^{-/-}$ mice (1, 2).

In contrast, the iNOS$^{-/-}$ mice, which only expressed eNOS, are protected during ischemia because eNOS produces only small amounts of NO. This low level of NO formation would not result in elevated levels of ONOO$^-$ because NO is the limiting factor in ONOO$^-$ formation where there is an excess of $O_2^{\cdot -}$ as is seen in galactosemia in all the mice. Thus, iNOS deficiency results in protection from the deleterious effects of galactosemia because there is no excess of NO in the presence of elevated levels of $O_2^{\cdot -}$. At the same time, there is no loss of "low level" NO production because eNOS is present and eNOS is "protective" to retinal endothelial cells.

By comparison, eNOS deficiency results in the expression of iNOS, which produces a high level of NO, thereby facilitating vasoconstriction as a result of reduced availability of NO due to ONOO$^-$ formation, increased leukocyte and platelet adhesion, and altered vascular pathology. The presence of galactosemia and laser injury accelerated the retinal pathology of the eNOS$^{-/-}$ mice, leading to even more aberrant retinal changes.

The increases in vascular NADH oxidase activity observed in galactose-induced retinopathy are comparable to those demonstrated in the BBZ/Wor rat model of spontaneous type II diabetes (12, 13). There were low levels of nitrotyrosine in the retinas of iNOS$^{-/-}$ mice despite the increase in NADH oxidase activity associated with the plasmalemma of astrocyte processes and with the vasculature. There was disruption of the basal infoldings in the RPE of the galactose-fed WT and eNOS$^{-/-}$ mice. Structural damage clearly appeared to be greater in these mice than in the iNOS$^{-/-}$ mice.

These findings implicate iNOS-generated NO as an important species in the generation of ONOO$^-$ and nitrotyrosine and subsequently the reduced bioavailability of NO in retinal pathology associated with diabetes.

Pilot studies of basement membrane thickening in galactose-induced diabetes demonstrated that the retinal capillary basement membranes of eNOS$^{-/-}$ mice on a diet of normal chow or 30% galactose were approximately twice as thick as those from age-matched WT and iNOS$^{-/-}$ mice on normal rodent chow or 30% galactose (11). These observations further support the deleterious effect of iNOS activation.

The low turnover rate of the retinal endothelium results in infrequent endothelial cell replacement in the absence of injury. Previously, we demonstrated that new retinal vessels are formed from circulating HSC and EPC in this laser-induced injury model (18). This model is suited for exploration of what dictates resident endothelial cell-driven versus HSC/EPC-driven vascular repair. In this model, donor-derived HSC/EPC significantly contribute to neovascularization. In the eNOS$^{-/-}$.gfp mice, the retinal vasculature, along with the vasculature of other unrelated organs, was entirely replaced with donor-derived WT EPC. The eNOS$^{-/-}$.gfp mice demonstrated dramatic incorporation of WT gfp$^+$ cells into newly forming preretinal vessels. Interestingly, these vessels were not patent and were never found perfused. However, copious amounts of new vessels were formed on the surface of the retina, and complete vascular tufts were made from the gfp$^+$ cells, without any contribution by the resident endothelial cells.

We conclude that resident endothelial cells in the eNOS$^{-/-}$ mice are in a state of chronic injury, releasing chemokines

such as stromal derived factor-1 and growth factors such as VEGF that facilitate the homing and repair by WT EPC in areas of injury. Widespread donor-derived HSC/EPC contributed to the retinal vasculature in the eNOS$^{-/-}$ recipients and formed dramatic preretinal neovascularization. We speculate based on this that the NO pathway may be critical in determining vascular repair following injury. In both physiological repair and pathological repair, HSC/EPC contribute to neovascularization. We also show that donor WT HSC transplanted into iNOS$^{-/-}$ recipients are functioning in an environment where local endothelial NO production is similar to what is seen in WT, due to the eNOS isoform that is expressed normally in iNOS$^{-/-}$ mice.

With our animal system, we can be confident about which NOS is the source of the NO generated, but not the actual amount of NO produced. Clearly, lacking the activity of one NOS isoform has significant consequences for HSC/EPC-driven neovascularization. Furthermore, although VEGF has been shown to be an upstream mediator of NO (35), these two pathways can function independently in neovascularization, because modification of the NO pathway independent of VEGF treatment affects blood-vessel formation, as is seen in eNOS$^{-/-}$ animals.

Our model provided WT HSC to the eNOS$^{-/-}$ animal, potentially correcting any stem cell defect present in these eNOS$^{-/-}$ mice. eNOS is essential for the functional activity of HSC/EPC. Defective mobilization of stem and progenitor cells contributes to the impairment of ischemia-induced neovascularization in eNOS$^{-/-}$ mice (1, 2) as eNOS$^{-/-}$ mice demonstrated impaired angiogenesis (29). Mice deficient in eNOS showed reduced activity of matrix metalloproteinase-9 (MMP-9) that may underlie the mobilization defect in eNOS$^{-/-}$ mice described by Aicher *et al*. (1, 2). This defect would not be present in the eNOS$^{-/-}$.gfp chimeric mice reconstituted with WT donor cells. Recent data identified MMP-9 as a major target for NO, which activates MMP-9 by *S*-nitrosylation (19) via ONOO$^-$. NO, either alone or in combination with reactive oxygen intermediates released by bone marrow cells after hematotoxic treatment such as chemotherapy, may participate in damage to bone marrow tissue.

In addition to regulating MMP-9, NO modulates proliferation, differentiation, and apoptosis in a variety of cell types (9, 29, 43). Aicher *et al.* postulated that endothelium-derived NO interferes with cell-cycle progression and/or differentiation of stem cells in the bone marrow (2). Papapetropoulos *et al*. demonstrated that autocrine production of NO appeared to be necessary for *in vitro* capillary tube formation, including vascular networks developing in response to VEGF (32, 33).

In conclusion, NO is a highly reactive molecule that can complex with the iron in heme-containing proteins, leading to inhibition of mitochondrial respiration, inhibition of DNA synthesis, and cytotoxicity. As shown in this study, NO can combine with reactive intermediates such as $O_2^{\cdot -}$, thereby generating additional toxic ONOO$^-$ and hydroxyl radicals that induce tissue injury. In addition to the toxic nature of ONOO$^-$, there is also a reduction in bioavailability of NO in the vascular endothelium where NO is known to play a significant role in vascular homeostasis. Reduction in the bioavailability of NO in the vascular endothelium occurs when there is an elevation of $O_2^{\cdot -}$ as a result of elevated levels of NADH oxidase and increased levels of NO generated by iNOS; this results in increased production of ONOO$^-$ (measured by nitrotyrosine) and occurs in hyperglycemia, galactosemia, ischemia, and hypoxia. Our studies support the critical participation of NO, which at physiological levels is the key modulator of normal vascular homeostasis, but at elevated levels can be associated with considerable vascular pathophysiology. The regulation of NOS activity as a means to influence the remodeling of vascular beds may provide specific treatment regimes, and this model is a useful system for investigating the NO pathway on hemangioblast activity.

ACKNOWLEDGMENTS

The work described was supported in part by NIH/NEI grants EY012601 and EY007739, and JDRF 4-2000-847.

ABBREVIATIONS

ANCOVA, analysis of covariance; BRB, blood–retinal barrier; DPI, diphenyleneiodonium; eNOS, endothelial NOS, also NOS3; EPC, endothelial precursor cell(s); FITC, fluorescein isothiocyanate; gfp, green fluorescent protein; H_2O_2, hydrogen peroxide; HSC, hematopoietic stem cell(s); iNOS, inducible NOS, also NOS2; MMP-9, matrix metalloproteinase-9 NIDDM, non–insulin-dependent diabetes mellitus; NO, nitric oxide; NOS, nitric oxide synthase; $O_2^{\cdot -}$, superoxide radical; ONOO$^-$, peroxynitrite; PBS, phosphate-buffered saline; ROS, reactive oxygen species; RPE, retinal pigment epithelium; SOD, superoxide dismutase; TBS, Tris-buffered saline buffer; VEGF, vascular endothelial growth factor; WT, wild type.

REFERENCES

1. Aicher A, Heeschen C, Mildner-Rihm C, Urbich C, Ihling C, Technau-Ihling K, Zeiher AM, and Dimmeler S. Essential role of endothelial nitric oxide synthase for mobilization of stem and progenitor cells. *Nat Med* 9: 1370–1376, 2003.
2. Aicher A, Heeschen C, and Dimmeler S. The role of NOS3 in stem cell mobilization. *Trends Mol Med* 10: 421–425, 2004.
3. Beckman JS and Koppenol WH. Nitric oxide, superoxide, and peroxytnitrite: the good, the bad, and the ugly. *Am J Physiol* 271: C1424–C1437, 1996.
4. Beckmann JS, Ye YZ, Anderson PG, Chen J, Accavitti MA, Tarpey MM, and White CR. Extensive nitration of protein tyrosines in human atherosclerosis detected by immunohistochemistry. *Biol Chem Hoppe Seyler* 375: 81–88, 1994.
5. Briggs RT, Karnovsky ML, and Karnovsky MJ. Hydrogen peroxide production in chronic granulomatous disease. A cytochemical study of reduced pyridine nucleotide oxidases. *J Clin Invest* 59: 1088–1098, 1977.
6. Carmo A, Cunha-Vaz JG, Carvalho AP, and Lopes MC. Nitric oxide synthase activity in retinas from non–insulin-

dependent diabetic Goto–Kakizaki rats: correlation with blood–retinal barrier permeability. *Nitric Oxide* 4: 590–596, 2000.
7. Chakravarthy U, Hayes RG, Stitt AW, McAuley E, and Archer DB. Constitutive nitric oxide synthase expression in retinal vascular endothelial cells is suppressed by high glucose and advanced glycation end products. *Diabetes* 47: 945–952, 1998.
8. Christ M, Bauersachs J, Liebetrau C, Heck M, Gunther A, and Wehling M. Glucose increases endothelial-dependent superoxide formation in coronary arteries by NAD(P)H oxidase activation: attenuation by the 3-hydroxy-3-methylglutaryl coenzyme A reductase inhibitor atorvastatin. *Diabetes* 51: 2648–2652, 2002.
9. Dimmeler S and Zeiher AM. Nitric oxide and apoptosis: another paradigm for the double-edged role of nitric oxide. *Nitric Oxide* 1: 275–281, 1997.
10. Du Y, Smith MA, Miller CM, and Kern TS. Diabetes-induced nitrative stress in the retina, and correction by aminoguanidine. *J Neurochem* 80: 771–779, 2002.
11. Ellis EA and Grant MB. Lack of vascular nitric oxide results in basement membrane thickening in galactose induced diabetic retinopathy. *Microsc Microanal* 11(Suppl 2): 1046 CD, 2005.
12. Ellis EA, Grant MB, Murray FT, Wachowski MB, Guberski DL, Kubilis PS, and Lutty GA. Increased NADH oxidase activity in the retina of the BBZ/Wor diabetic rat. *Free Radic Biol Med* 24: 111–120, 1998.
13. Ellis EA, Guberski DL, Somogyi-Mann M, and Grant MB. Increased H_2O_2, vascular endothelial growth factor and receptors in the retina of the BBZ/Wor diabetic rat. *Free Radic Biol Med* 28: 91–101, 2000.
14. Ellis EA, Guberski DL, Hutson B, and Grant MB. Time course of NADH oxidase, inducible nitric oxide synthase and peroxynitrite in diabetic retinopathy in the BBZ/WOR rat. *Nitric Oxide* 6: 295–304, 2002.
15. El-Remessy AB, Behzadian MA, Abou-Mohamed G, Franklin T, Caldwell RW, and Caldwell RB. Experimental diabetes causes breakdown of the blood–retina barrier by a mechanism involving tyrosine nitration and increases in expression of vascular endothelial growth factor and urokinase plasminogen activator receptor. *Am J Pathol* 162: 1995–2004, 2003.
16. Gorlach A, Diebold I, Schini-Kerth VB, Berchner-Pfannschmidt U, Roth U, Brandes RP, Kietzmann T, and Busse R. Thrombin activates the hypoxia-inducible factor-1 signaling pathway in vascular smooth muscle cells: role of the p22(phox)-containing NADPH oxidase. *Circ Res* 89: 47–54, 2001.
17. Goyal P, Weissmann N, Grimminger F, Hegel C, Bader L, Rose F, Fink L, Ghofrani HA, Schermuly RT, Schmidt HH, Seeger W, and Hanze J. Upregulation of NAD(P)H oxidase 1 in hypoxia activates hypoxia-inducible factor 1 via increase in reactive oxygen species. *Free Radic Biol Med* 36: 1279–1288, 2004.
18. Grant MB, May WS, Caballero S, Brown GA, Guthrie SM, Mames RN, Byrne BJ, Vaught T, Spoerri PE, Peck AB, and Scott EW. Adult hematopoietic stem cells provide functional hemangioblast activity during retinal neovascularization. *Nat Med* 8: 607–612, 2002.
19. Gu Z, Kaul M, Yan B, Kridel SJ, Cui J, Strongin A, Smith JW, Liddington RC, and Lipton SA. *S*-Nitrosylation of matrix metalloproteinases: signaling pathway to neuronal cell death. *Science* 297: 1186–1190, 2002.
20. Hardy P, Dumont I, Bhattacharya M, Hou X, Lachapelle P, Varma DR, and Chemtob S. Oxidants, nitric oxide and prostanoids in the developing ocular vasculature: a basis for ischemic retinopathy. *Cardiovasc Res* 47: 489–509, 2000.
21. Ignarro LJ. Nitric oxide. A novel signal transduction mechanism for transcellular communication. *Hypertension* 16: 477–483, 1990.
22. Kern TS and Engerman RL. Comparison of retinal lesions in alloxan-diabetic rats and galactose-fed rats. *Curr Eye Res* 13: 863–867, 1994.
23. Kern TS and Engerman RL. A mouse model of diabetic retinopathy. *Arch Ophthalmol* 114: 986–990, 1996.
24. Kim YK, Lee MS, Son SM, Kim IJ, Lee WS, Rhim BY, Hong KW, and Kim CD. Vascular NADH oxidase is involved in impaired endothelium-dependent vasodilation in OLETF rats, a model of type 2 diabetes. *Diabetes* 51: 522–527, 2002.
25. Kossenjans W, Eis A, Sahay R, Brockman D, and Myatt L. Role of peroxynitrite in altered fetal–placental vascular reactivity in diabetes or preeclampsia. *Am J Physiol Heart Circ Physiol* 278: H1311–H1319, 2000.
26. Lassegue B and Clempus RE. Vascular NAD(P)H oxidases: specific features, expression, and regulation. *Am J Physiol Regul Integr Comp Physiol* 285: R277–R297, 2003.
27. Mohazzab KM, Kaminski PM, and Wolin MS. NADH oxidoreductase is a major source of superoxide anion in bovine coronary artery endothelium. *Am J Physiol* 266: H2568–H2572, 1994.
28. Moncada S and Higgs A. The L-arginine–nitric oxide pathway. *N Engl J Med* 329: 2002–2012, 1993.
29. Murohara T, Asahara T, Silver M, Bauters C, Masuda H, Kalka C, Kearney M, Chen D, Symes JF, Fishman MC, Huang PL, and Isner JM. Nitric oxide synthase modulates angiogenesis in response to tissue ischemia. *J Clin Invest* 101: 2567–2578, 1998.
30. Murohara T, Witzenbichler B, Spyridopoulos I, Asahara T, Ding B, Sullivan A, Losordo DW, and Isner JM. Role of endothelial nitric oxide synthase in endothelial cell migration. *Arterioscler Thromb Vasc Biol* 19: 1156–1161, 1999.
31. Osborne NN, Casson RJ, Wood JP, Chidlow G, Graham M, and Melena J. Retinal ischemia: mechanisms of damage and potential therapeutic strategies. *Prog Retin Eye Res* 23: 91–147, 2004.
32. Papapetropoulos A, Desai KM, Rudic RD, Mayer B, Zhang R, Ruiz-Torres MP, Garcia-Cardena G, Madri JA, and Sessa WC. Nitric oxide synthase inhibitors attenuate transforming-growth-factor-beta 1-stimulated capillary organization in vitro. *Am J Pathol* 150: 1835–1844, 1997.
33. Papapetropoulos A, Garcia-Cardena G, Madri JA, and Sessa WC. Nitric oxide production contributes to the angiogenic properties of vascular endothelial growth factor in human endothelial cells. *J Clin Invest* 100: 3131–3139, 1997.
34. Rajagopalan S, Kurz S, Munzel T, Tarpey M, Freeman BA, Griendling KK, and Harrison DG. Angiotensin II-mediated hypertension in the rat increases vascular superoxide

production via membrane NADH/NADPH oxidase activation. Contribution to alterations of vasomotor tone. *J Clin Invest* 97: 1916–1923, 1996.
35. Risau W. Mechanisms of angiogenesis. *Nature* 386: 671–674, 1997.
36. Robison WG Jr, Kador PF, and Kinoshita JH. Retinal capillaries: basement membrane thickening by galactosemia prevented with aldose reductase inhibitor. *Science* 221: 1177–1179, 1983.
37. Salerno L, Sorrenti V, Di Giacomo C, Romeo G, and Siracusa MA. Progress in the development of selective nitric oxide synthase (NOS) inhibitors. *Curr Pharm Des* 8: 177–200, 2002.
38. Smith LE, Wesolowski E, McLellan A, Kostyk SK, D'Amato R, Sullivan R, and D'Amore PA. Oxygen-induced retinopathy in the mouse. *Invest Ophthalmol Vis Sci* 35: 101–111, 1994.
39. Sobrevia L and Mann GE. Dysfunction of the endothelial nitric oxide signalling pathway in diabetes and hyperglycaemia. *Exp Physiol* 82: 423–452, 1997.
40. Sonta T, Inoguchi T, Tsubouchi H, Sekiguchi N, Kobayashi K, Matsumoto S, Utsumi H, and Nawata H. Evidence for contribution of vascular NAD(P)H oxidase to increased oxidative stress in animal models of diabetes and obesity. *Free Radic Biol Med* 37: 115–123, 2004.
41. Tannous M, Rabini RA, Vignini A, Moretti N, Fumelli P, Zielinski B, Mazzanti L, and Mutus B. Evidence for iNOS-dependent peroxynitrite production in diabetic platelets. *Diabetologia* 42: 539–544, 1999.
42. Williamson JR, Chang K, Frangos M, Hasan KS, Ido Y, Kawamura T, Nyengaard JR, van den Enden M, Kilo C, and Tilton RG. Hyperglycemic pseudohypoxia and diabetic complications. *Diabetes* 42: 801–813, 1993.
43. Ziche M, Morbidelli L, Masini E, Amerini S, Granger HJ, Maggi CA, Geppetti P, and Ledda F. Nitric oxide mediates angiogenesis in vivo and endothelial cell growth and migration in vitro promoted by substance P. *J Clin Invest* 94: 2036–2044, 1994.

Address reprint requests to:
M.B. Grant, M.D.
Department of Pharmacology
Box 100267
Gainesville, FL 32610-0267

E-mail: grantma@pharmacology.ufl.edu

Received for publication June 20, 2005; accepted June 30, 2005.

This article has been cited by:

1. Carl A. Hubel, Peter I. Sipos, Ian P. Crocker. 2011. Endothelial progenitor cells: Their potential role in pregnancy and preeclampsia. *Pregnancy Hypertension: An International Journal of Women's Cardiovascular Health* **1**:1, 48-58. [CrossRef]
2. Sun-Jung Kim, Myung-Sin Lim, Soo-Kyung Kang, Yong-Soon Lee, Kyung-Sun Kang. 2008. Impaired functions of neural stem cells by abnormal nitric oxide-mediated signaling in an in vitro model of Niemann-Pick type C disease. *Cell Research* **18**:6, 686-694. [CrossRef]
3. L. Zheng, Y. Du, C. Miller, R. A. Gubitosi-Klug, T. S. Kern, S. Ball, B. A. Berkowitz. 2007. Critical role of inducible nitric oxide synthase in degeneration of retinal capillaries in mice with streptozotocin-induced diabetes. *Diabetologia* **50**:9, 1987-1996. [CrossRef]
4. Nicanor I. Moldovan . 2005. Emerging Roles of Reactive Oxygen and Nitrogen Species in Stem/Progenitor Cells. *Antioxidants & Redox Signaling* **7**:11-12, 1409-1412. [Citation] [Full Text PDF] [Full Text PDF with Links]